Research Article | Vol. 27, No. 19 / 16 September 2019 / Optics Express 27076
Optics EXPRESS

Optically mutual-injected terahertz quantum cascade lasers for self-mixing velocity measurements

YUANYUAN LI,[1] WEIDONG CHU,[1] NING YANG,[1,*] LEI GE,[1] YAN XIE,[2] WEI ZHANG,[1] SUQING DUAN,[1] YINGXIN WANG,[2] AND JIALIN SUN[3]

[1]Institute of Applied Physics and Computational Mathematics, Beijing, 100088, China
[2]Department of Engineering Physics, Tsinghua University, Beijing, 100084, China
[3]Department of Physics, Tsinghua University, Beijing, 100084, China
[*]yang_ning@iapcm.ac.cn

Abstract: Self-mixing velocity sensor based on a mutual-injected two-element terahertz quantum cascade laser (THz QCL) array is studied theoretically. The working characteristics of mutual-injected THz QCL array with different frequency detunings and self-mixing feedback strengths, as well as their influences on the self-mixing measurements are discussed in detail. Within the phase-locked range, each laser in the array reaches a stable state rapidly and can be used as a self-mixing detector due to the mutual injection coupling. The array will no longer be phase-locked when the frequency detuning of the lasers is too large, and only the laser that receives the feedback light can still be used for self-mixing velocity measurements. It is also found that even for the case of strong feedback, the THz QCLs will not be completely unstable and the self-mixing velocity measurements could also be possible. In addition, the simulation also shows that the array could measure two independent moving targets simultaneously. These results provide the theoretical support for the future applications of THz QCL arrays in self-mixing sensors.

© 2019 Optical Society of America under the terms of the OSA Open Access Publishing Agreement

1. Introduction

Terahertz (THz) imaging and sensing technology has broad application prospects in materials analysis, industrial control, biomedical sensing, security screening, fireground detection, and other fields [1–3]. Terahertz quantum cascade lasers (THz QCLs) are important semiconductor sources of terahertz radiation and have been used in varieties of THz imaging and sensing systems [4,5].

Self-mixing interference is an important laser imaging and sensing technique which is manifested in a modulation of laser power and emission frequency when a fraction of the emitted light reflected by an external target is reinjected into the laser cavity [6]. THz QCLs are more stable under strong optical injection and high-frequency modulation than diode lasers due to the smaller linewidth enhancement factor of $0.1 \sim 0.5$ and shorter carrier lifetimes of several picoseconds [7,8]. Then THz QCLs are very suitable light sources for self-mixing interference systems. In recent years, the self-mixing interference measurements based on THz QCLs have been widely applied in terahertz imaging, vibration sensor, and velocity measurements [5,9]. The resolution of displacement measurement has achieved $\lambda/1000$ with a hybrid THz QCLs system based on the self-mixing of THz QCLs and the near field technique [10]. Moreover, the simultaneous measurement of two independent moving targets by the self-mixing interference of a single QCL has been demonstrated [11].

However, the low power and poor beam quality of a single THz QCL device limit long-distance self-mixing measurements. In recent years, array technologies including tree array [12], ring array [13], antenna mutual coupling array [14], surface-emitting array [15], and π coupling array

#372126 https://doi.org/10.1364/OE.27.027076
Journal © 2019 Received 8 Jul 2019; revised 14 Aug 2019; accepted 16 Aug 2019; published 11 Sep 2019

Optics EXPRESS

[16] have been employed to improve the power of THz QCLs while maintaining the spectral purity. A phase-locked THz QCL array with higher output power and better beam quality may be suitable for long-distance self-mixing measurements. In addition, the 2D/3D imaging speed of self-mixing imaging systems based on scanning imaging is still very slow, and the multi-target self-mixing imaging based on THz QCL arrays combined with a fast scanning mirror could be of great help for fast imaging systems [17].

The optically mutual-injected array is one of the most common array technologies, and it has abundant dynamics under different working conditions including basic phase-locking properties [18], slow stairs-like periodic modulation [19], symmetry-breaking [20], and chaos synchronization [21,22]. Since the dynamical behaviors of a laser array are much more complex than an individual laser, its response rules to the self-mixing feedback would also vary with the working conditions. Although significant progress has been made in phase-locked THz QCL arrays recently, studies of the properties of THz QCL arrays with self-mixing feedback are still limited. Then we will take a mutual-injected THz QCL array as an example to study the basic characteristics of self-mixing interference and multi-target sensing with THz QCL arrays.

In this study, we are mainly concerned with the basic properties of self-mixing interference within and out of the phase-locked region of the THz QCL array and the possibility of the self-mixing velocity measurements. The phase-locked range of the array is deduced, and the influences of frequency detuning, self-mixing feedback strength, and the target's displacement on the self-mixing signals are simulated. The results show that mutual-injected THz QCL arrays can realize self-mixing velocity measurements under different working conditions, and can be extended to measure two targets simultaneously, which are helpful for applications in laser self-mixing interferometer.

2. Theoretical model

We consider three different geometries of mutual-injected laser arrays with self-mixing feedbacks. The schematic diagram of the self-mixing interferometer based on a face-to-face mutual-injected THz QCLs is shown in Figs. 1(a) and 1(b), which correspond to the cases of one and two external reflective targets, respectively. Experimentally coupled lasers usually produce a combined beam containing components from each laser. So the feedback light from each target may be re-injected into two lasers at the same time and the corresponding schematic diagram is shown in Fig. 1(c).

THz QCLs A and B are two mutual-injected laser sources. Target A and target B are two independent moving targets with velocities v_{TA} and v_{TB}, respectively. The dynamics of a THz QCL under optical feedback can be described by the Lang-Kobayashi equations [23], which can be extended to characterize our model. Take the case of Fig. 1(a) as an example, the rate equations are written as:

$$\frac{d\varepsilon_A(t)}{dt} = i\Omega_{A0}\varepsilon_A(t) + \frac{1}{2}(1+i\alpha)\{Zg[N_{A,3}(t) - N_{A,2}(t)] - \frac{1}{\tau_p}\}\varepsilon_A(t) + \frac{\kappa_c}{\tau_l}\varepsilon_B(t-\tau_{ext}) + \frac{\kappa_{OL}}{\tau_l}\varepsilon_A(t-\tau_{OL}), \tag{1}$$

$$\frac{d\varepsilon_B(t)}{dt} = i\Omega_{B0}\varepsilon_B(t) + \frac{1}{2}(1+i\alpha)\{Zg[N_{B,3}(t) - N_{B,2}(t)] - \frac{1}{\tau_p}\}\varepsilon_B(t) + \frac{\kappa_c}{\tau_l}\varepsilon_A(t-\tau_{ext}), \tag{2}$$

$$\frac{dN_{A,3}(t)}{dt} = \frac{I_{in,A}}{q} - \frac{N_{A,3}(t)}{\tau_{32}} - \frac{N_{A,3}(t)}{\tau_{31}} - g[N_{A,3}(t) - N_{A,2}(t)]|\varepsilon_A(t)|^2, \tag{3}$$

$$\frac{dN_{B,3}(t)}{dt} = \frac{I_{in,B}}{q} - \frac{N_{B,3}(t)}{\tau_{32}} - \frac{N_{B,3}(t)}{\tau_{31}} - g[N_{B,3}(t) - N_{B,2}(t)]|\varepsilon_B(t)|^2, \tag{4}$$

$$\frac{dN_{A,2}(t)}{dt} = \frac{N_{A,3}(t)}{\tau_{32}} - \frac{N_{A,2}(t)}{\tau_{21}} + g[N_{A,3}(t) - N_{A,2}(t)]|\varepsilon_A(t)|^2, \tag{5}$$

Optics EXPRESS

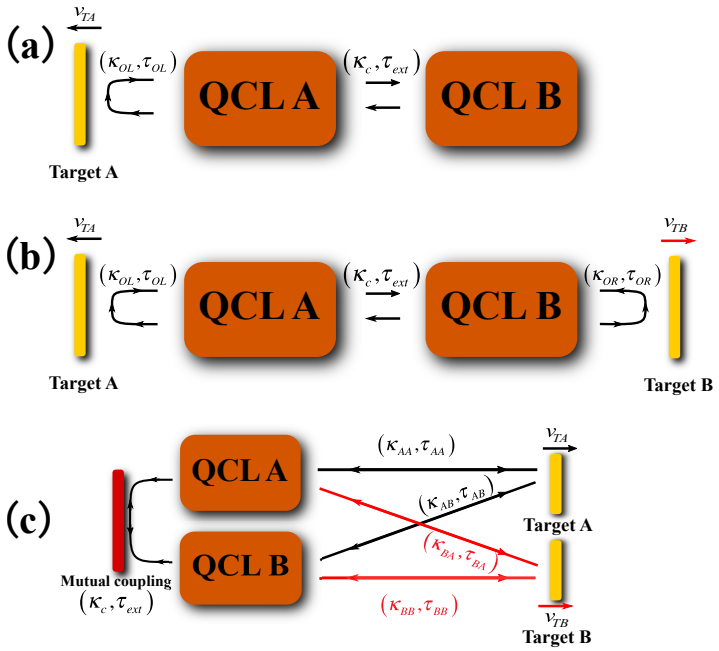

Fig. 1. The schematic diagram of the self-mixing velocity measurements for (a) one target and (b) two targets based on two face-to-face mutual-injected THz QCLs. (c) Two mutual-injected THz QCLs receive feedback lights from two targets at the same time.

$$\frac{dN_{B,2}(t)}{dt} = \frac{N_{B,3}(t)}{\tau_{32}} - \frac{N_{B,2}(t)}{\tau_{21}} + g[N_{B,3}(t) - N_{B,2}(t)]|\varepsilon_B(t)|^2, \tag{6}$$

$$\frac{dN_{A,1}(t)}{dt} = \frac{N_{A,3}(t)}{\tau_{31}} + \frac{N_{A,2}(t)}{\tau_{21}} - \frac{N_{A,1}(t)}{\tau_{out}}, \tag{7}$$

$$\frac{dN_{B,1}(t)}{dt} = \frac{N_{B,3}(t)}{\tau_{31}} + \frac{N_{B,2}(t)}{\tau_{21}} - \frac{N_{B,1}(t)}{\tau_{out}}. \tag{8}$$

For one single period of the active region in QCL A/B, we denote the instantaneous carrier numbers in the upper, lower laser state, and the collector state by $N_{A/B,3}$, $N_{A/B,2}$, and $N_{A/B,1}$ respectively. $\varepsilon_{A/B}$ is the complex electric field of QCL A/B. Ω_{A0} and Ω_{B0} are the cavity resonance frequencies of the two free-running lasers without mutual injection and feedback. α denotes the linewidth enhancement factor and τ_p is the photon lifetime in the active region. g is the optical differential gain coefficient of the active region, and Z is the number of stages of a THz QCL. κ_c is the mutual injection coupling strength of the two QCLs. κ_{OL} and κ_{OR} are the self-mixing feedback strengths of targets A and B, respectively. The round-trip time for light in the laser cavity τ_l is calculated from $\tau_l = 2nL/c$, where n is the effective refractive index of the laser cavity and L is the length of the laser cavity. $I_{in,A/B} = \eta(1 + a)I_{th}$ is the effective current injected into the active region of QCL A/B, where η, a, and I_{th} are the injection efficiency, pump parameter, and threshold current, respectively. It is noted that the continuity of the injected current is required according to the operation principle of QCL, i.e., $I_{in,A/B}/q = N_{A/B,1}/\tau_{out}$ with τ_{out} being the lifetime of carriers out of level 1 into the subsequent miniband [24]. τ_{32}, τ_{31}, and τ_{21} represent the lifetimes between the laser levels.

For Figs. 1(a) and 1(b), the spatial distance between the two coupled lasers is defined as d. $L_{OL/OR}$ represents the instantaneous distance between the QCL A/B and the corresponding target A/B. It is assumed that the devices work in a vacuum environment. So the corresponding

Optics EXPRESS

delay times are given by $\tau_{ext} = d/c$, $\tau_{OL} = 2L_{OL}/c = 2(L_{0,OL} + v_{TA}t)/c$, and $\tau_{OR} = 2L_{OR}/c = 2(L_{0,OR}+v_{TB}t)/c$, where $L_{0,OL}$ and $L_{0,OR}$ are the initial position of targets A and B respectively. The key parameters in the simulations are listed in Table 1, if not specified. We consider such a simple case that QCLs A and B have exactly the same parameters except for the free-running frequency. Then, we could verify the feasibility of self-mixing measurements and the characteristics of the array under different working conditions.

Table 1. Values of key parameters used in the simulations.

Symbol	Quantity	Value
$\Omega_{B0}/2\pi$	Stationary emission frequency of free-running QCL B	2.5 THz
v_{TA}	Velocity of target A	60 mm/s
v_{TB}	Velocity of target B	600 mm/s
L	Length of the laser cavity	3 mm [25]
d	Distance between the light-emitting facets of two QCLs	0.1 m
n	Effective refractive index of the laser cavity	3.61 [26]
κ_c	Coupling strength of QCLs A and B	7.983×10^{-2}
τ_p	Photon lifetime	3.7 ps [25]
τ_{32}	Photon scattering time ($3 \rightarrow 2$)	2 ps [25]
τ_{31}	Photon scattering time ($3 \rightarrow 1$)	2.4 ps [25]
τ_{21}	Photon scattering time ($2 \rightarrow 1$)	0.3 ps [25]
$L_{0,OL}$	The initial distance between target A and QCL A	1 m
$L_{0,OR}$	The initial distance between target B and QCL B	1 m
g	Differential gain coefficient	3.46×10^3 s^{-1}
Z	Number of the stages of QCL A/B	100
α	Linewidth enhancement factor	0.1 [27,28]
I_{th}	Threshold current	300 mA [29,30]
η	Injection efficiency	0.45
a	Pump parameter	1.6
$I_{in,A}, I_{in,B}$	Effective injection current	351 mA
q	Electron charge	1.602×10^{-19} C

For the case of Fig. 1(c), the real geometry of the array could be complex, but here the effective coupling κ_c and delay time τ_c are employed to model the real mutual injection of the optical fields. $\kappa_{AA}(\tau_{AA})$, $\kappa_{AB}(\tau_{AB})$, $\kappa_{BA}(\tau_{BA})$, and $\kappa_{BB}(\tau_{BB})$ are optical feedback strengths (delay times) from the targets to the lasers, respectively. Considering that the targets are usually far from the laser array, we assume that $\kappa_{AA} = \kappa_{AB} \equiv \kappa_A$, $\kappa_{BA} = \kappa_{BB} \equiv \kappa_B$, $\tau_{AA} = \tau_{AB} = 2(L_{0,OL} + v_{TA}t)/c \equiv \tau_A$, and $\tau_{BA} = \tau_{BB} = 2(L_{0,OR} + v_{TB}t)/c \equiv \tau_B$.

First we study the situation in Fig. 1(a) and discuss the conditions under which the THz QCL array can maintain phase-locked operation with optical feedback. If the THz QCL array achieves phase locking operation under external feedback, the complex electric fields will have the following form:

$$\varepsilon_A(t) = F_A \exp(i\omega_L t), \qquad \varepsilon_B(t) = F_B \exp(i\omega_L t + i\phi_L), \tag{9}$$

where F_A and F_B are the electric field amplitudes of QCL A and QCL B, respectively. ω_L is the phase-locked frequency and ϕ_L is the corresponding phase difference. By substituting Eq. (9)

Optics EXPRESS

into Eqs. (1) and (2), it can be obtained:

$$\begin{aligned} 0 = \Omega_{A0} - \omega_L - \frac{\kappa_c}{\tau_l}\frac{F_B}{F_A}\sqrt{1+\alpha^2}\sin(\omega_L\tau_{ext} - \phi_L + \arctan\alpha) \\ - \frac{\kappa_{OL}}{\tau_l}\sqrt{1+\alpha^2}\sin(\omega_L\tau_{OL} + \arctan\alpha), \end{aligned} \tag{10}$$

$$0 = \Omega_{B0} - \omega_L - \frac{\kappa_c}{\tau_l}\frac{F_A}{F_B}\sqrt{1+\alpha^2}\sin(\omega_L\tau_{ext} + \phi_L + \arctan\alpha). \tag{11}$$

Eqs. (10) and (11) are two coupled transcendental equations, and it is difficult to solve ϕ_L and ω_L directly. When the feedback strength κ_{OL} and the coupling strength κ_c are quite small, the right-hand sides of Eqs. (10) and (11) are monotonic functions of ω_L for arbitrary ϕ_L, which will result in at least one solution. We substitute Eq. (11) into Eq. (10) to obtain the following expressions for the frequency detuning $\Delta\Omega = \Omega_{B0} - \Omega_{A0}$:

$$\begin{aligned} \Delta\Omega = \frac{\kappa_c}{\tau_l}\frac{F_A}{F_B}\sqrt{1+\alpha^2}\sin(\omega_L\tau_{ext} + \phi_L + \arctan\alpha) \\ - \frac{\kappa_c}{\tau_l}\frac{F_B}{F_A}\sqrt{1+\alpha^2}\sin(\omega_L\tau_{ext} - \phi_L + \arctan\alpha) \\ - \frac{\kappa_{OL}}{\tau_l}\sqrt{1+\alpha^2}\sin(\omega_L\tau_{OL} + \arctan\alpha). \end{aligned} \tag{12}$$

According to the boundedness of the trigonometric function, the maximum allowable frequency detuning for the existence of phase-locked solutions is

$$|\Delta\Omega|_{max} = (\kappa_c\frac{F_B}{F_A} + \kappa_c\frac{F_A}{F_B} + \kappa_{OL})\frac{\sqrt{1+\alpha^2}}{\tau_l}. \tag{13}$$

Since the parameters of the two lasers are identical except for the frequency, $F_A = F_B$ can be considered as a general approximation. Then the phase-locked range of the mutual-injected THz QCL array can be expressed as:

$$|\Delta\Omega|_{max} = (2\kappa_c + \kappa_{OL})\frac{\sqrt{1+\alpha^2}}{\tau_l}. \tag{14}$$

For the case of weak feedback strength κ_{OL}, Eq. (14) shows that the phase-locked range of the array increases with κ_{OL} and κ_c, which is similar to the phase-locked range of the mutual-injected array [18]. In fact, the working state of the lasers varies with the coupling strength κ_c, feedback strength κ_{OL}, and the instantaneous position of the moving target. To clearly show the operating characteristics of the QCLs, we will analyze the dependences of the working state of the lasers on those parameters by numerical simulations of Eqs. (1)–(8) and discuss the results in the following section.

3. Simulation and discussion

To simulate the properties of THz QCL arrays with one moving target in Fig. 1(a), the case of weak self-mixing feedback strength is considered first. Without loss of generality, we always keep Ω_{B0} unchanged and only change the frequency of QCL A in simulations. Within the phase-locked range determined by Eq. (14), a typical simulation result of the time evolution of Eqs. (1)–(8) with $\Delta\Omega/2\pi = 0.1$ GHz and $\kappa_{OL} = 0.1\kappa_c$ are shown in Fig. 2. Figure 2(a) shows the time evolution of inversion population $N_{A/B} = N_{A/B,3} - N_{A/B,2}$ with fixed target's displacements $\Delta L_A = v_{TA}t = 40\ \mu m$ and $120\ \mu m$. It is found that after a short time of interaction, N_A and N_B rapidly reach their final steady states. For target with low velocity, the sampling interval of

Optics EXPRESS

velocity measurements is much longer than the time for QCLs to reach steady states. In our simulations, the sampling interval of self-mixing measurements is 12.5 μs, which is much longer than the time required for lasers' stabilization (˜15 ns in Fig. 2(a)). Then we take the average values of $N_{A/B}$ over 20 ns after they arrive at the steady states (from 20 ns to 40 ns in Fig. 2(a)) as the self-mixing signals of the moving target at any position. The optical gain of QCL A/B can be expressed as $ZgN_{A/B}$, so the change in gain and output power of the laser is proportional to the change in the inversion population. In self-mixing experiments, the variations in voltage offset at the QCL's terminals are just proportional to the variations in output power. So the variations in inversion population of QCL A/B are proportional to the variations in terminal voltage and are always taken as the measurable self-mixing signals [11].

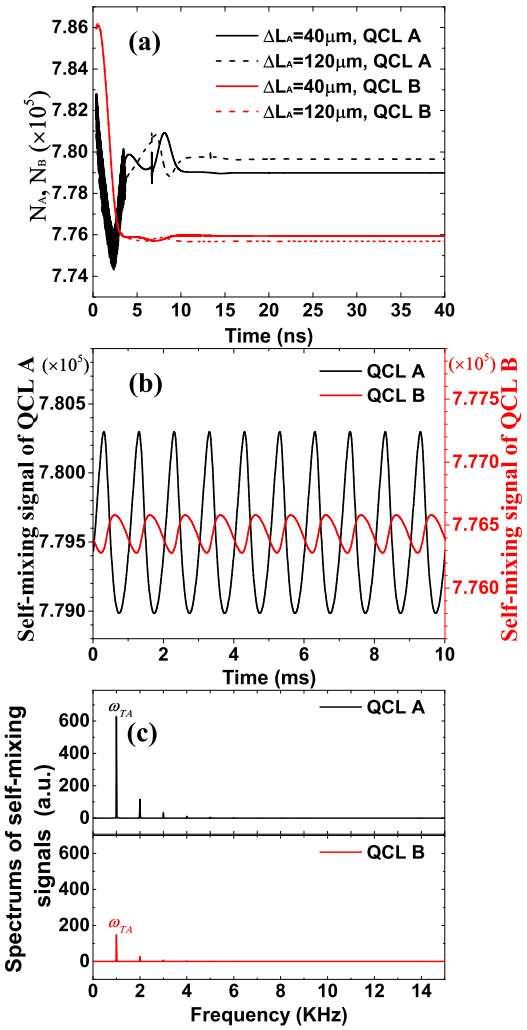

Fig. 2. The simulation of the phase-locked THz QCL array with frequency detuning $\Delta\Omega/2\pi = 0.1$ GHz and feedback strength $\kappa_{OL} = 0.1\kappa_c$. (a) Time evolution of $N_{A/B}$ with $\Delta L_A = 40\mu m$ and $120\mu m$, (b) the self-mixing signals given by QCLs A and B with moving target $v_{TA} = 60$ mm/s, (c) spectrums of self-mixing signals.

The simulated self-mixing signals of QCLs A and B with the moving target are plotted in Fig. 2(b). It is found that although the feedback light reflected by target A is only injected into

Optics EXPRESS

QCL A, the self-mixing signals of both lasers fluctuate as the target moves. It means that the optical feedback of any laser in the array is manifested in the whole array.

From Eqs. (1)–(6) and the form of the steady state solutions Eq. (9), the stable solutions for the inversion populations N_A and N_B could be obtained as

$$N_A = \frac{1}{Zg}[-2\frac{\kappa_c}{\tau_l}\frac{F_B}{F_A}\cos(\omega_L\tau_{ext} - \phi_L) - 2\frac{\kappa_{OL}}{\tau_l}\cos(\omega_L\frac{2L_{0,OL}}{c} + \omega_{TA}t) + \frac{1}{\tau_p}], \tag{15}$$

$$N_B = \frac{1}{Zg}[-2\frac{\kappa_c}{\tau_l}\frac{F_A}{F_B}\cos(\omega_L\tau_{ext} + \phi_L) + \frac{1}{\tau_p}], \tag{16}$$

where $\omega_{TA} = 2\omega_L v_{TA}/c$ is the Doppler frequency of target A. This implies that N_A contains the information about the velocity of target A which could be extracted by the Fourier transform.

Figure 2(c) shows the Fourier transform of the self-mixing signal $N_{A/B}$ in Fig. 2(b). For clarity, we only show the non-zero frequency component of the self-mixing signal spectrums. From the Fourier transform spectrums in Fig. 2(c), it can be identified that in both of the spectrums of QCLs A and B, the first main peak 1 KHz corresponds to $\omega_{TA} = 2\Omega_L v_{TA}/c$. Therefore, the main peaks of the self-mixing signal spectrums of both QCLs A and B can be employed to identify the target's velocity v_{TA}, except that the main peak intensities for QCLs A and B are different. This is reasonable because the two lasers keep phase-locked with the motion of the targets through the mutual injection coupling.

It should be noted that for a higher velocity of the target A, the smaller sampling interval is needed to ensure that the spectrum range of self-mixing signal covers the Doppler frequency ω_{TA}. When the sampling interval approaches the laser response time, the self-mixing measurement cannot be carried out. Because of the ultra-fast dynamics of THz QCLs relative to diode lasers, THz QCLs may be applied to higher-speed measurements.

It has been known that the array cannot be phase-locked when the frequency detuning is too large and each laser in the array is equivalent to a modulator for the other laser [18]. For this case, the simulation of self-mixing measurement with $\Delta\Omega/2\pi = 10$ GHz is carried out, and the simulated results are shown in Fig. 3. Figure 3(a) shows that the inversion populations of both lasers oscillate rapidly with time even with a fixed target, but the amplitudes are quite small compared with their average values. The frequency of the oscillation of $N_{A/B}$ just equals to the detuning frequency 10 GHz and its origin had been discussed in [18]. Since the oscillation frequency of $N_{A/B}$ is much larger than the Doppler frequency $\omega_{TA}/2\pi = 1$ KHz, the self-mixing signals with the moving target can be obtained by the same method as Fig. 2(b) and are shown in Fig. 3(b), except that the averaging interval is from 0.2 ns to 10 ns. It is found that the self-mixing signal of QCL A with the moving target still oscillates with time, while the self-mixing signal of laser B tends to be stable. Then, as demonstrated in Fig. 3(c), only the main peak of the self-mixing signal spectrum of QCL A corresponds to ω_{TA}. It means that the coupling of the two lasers is destroyed by the large frequency detuning and only the self-mixing signal of QCL A contains the velocity information of the target.

So far, we have demonstrated the possibility of self-mixing velocity measurements with THz QCL array under weak optical feedback. For the case of strong feedback strength, the simulation results with the fixed target's displacements ΔL_A of 40μ m and 80μm, $\kappa_{OL} = 0.4\kappa_c$, and $\Delta\Omega/2\pi$ =0.16 GHz are shown in Fig. 4(a). It can be found that the oscillating pattern of the inversion population $N_{A/B}$ varies greatly for $\Delta L_A = 40\mu$m and 80μm. However, $N_{A/B}$ appears to be periodic and never exhibits extreme instability. The self-mixing signals of the moving target (obtained by averaging $N_{A/B}$ from 20 ns to 100 ns in Fig. 4(a)) are shown in Fig. 4(b). The results show that the self-mixing signals have obvious periodicity, but they become complex compared with Figs. 2(b) and 3(b). As shown in Fig. 4(c), further analysis of the spectrums of the self-mixing signals indicates that the main peak corresponding to ω_{TA} can still be found for both of lasers, but the main peak is no longer sharp and the spectrums are distributed in a wide

Optics EXPRESS

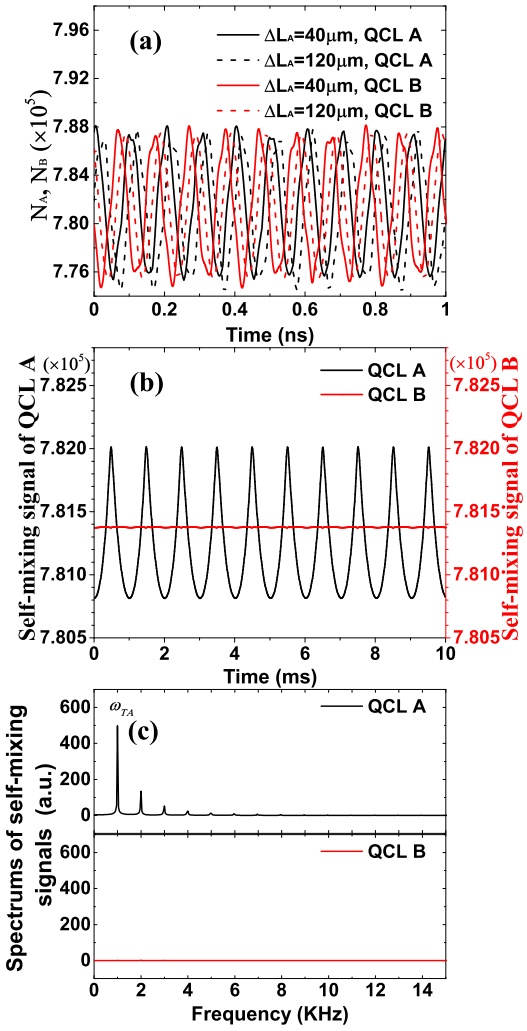

Fig. 3. Out of the phase-locked range, the simulation of THz QCL array with frequency detuning $\Delta\Omega/2\pi = 10$ GHz and feedback strength $\kappa_{OL} = 0.1\kappa_c$. (a) Time evolution of $N_{A/B}$ with $\Delta L_A = 40\mu m$ and $\Delta L_A = 120\mu m$, (b) the self-mixing signals of QCLs A and B with the moving target $v_{TA} = 60$ mm/s, (c) spectrums of self-mixing signals.

frequency range. It means that THz QCL array may still be used for self-mixing measurements under strong feedback, although the spectral resolution of the self-mixing signal is reduced. In fact, the cases with much larger feedback strengths κ_{OL} (up to $20\kappa_c$) are also simulated and compared with those of diode lasers. The results show that THz QCL arrays are more stable than diode laser arrays under strong feedback, and the self-mixing velocity measurements can still be performed.

As discussed above, the target's velocity can be obtained from the self-mixing signal of each laser if the array is phase-locked. Recently, the simultaneous velocity measurements of two independent targets based on a single QCL have been demonstrated [11]. It inspires us to study whether mutual injection arrays can simultaneously measure two independent targets. We add a target B with velocity v_{TB} to our model, as shown in Fig. 1(b). Correspondingly, Eq. (2) will be

Optics EXPRESS

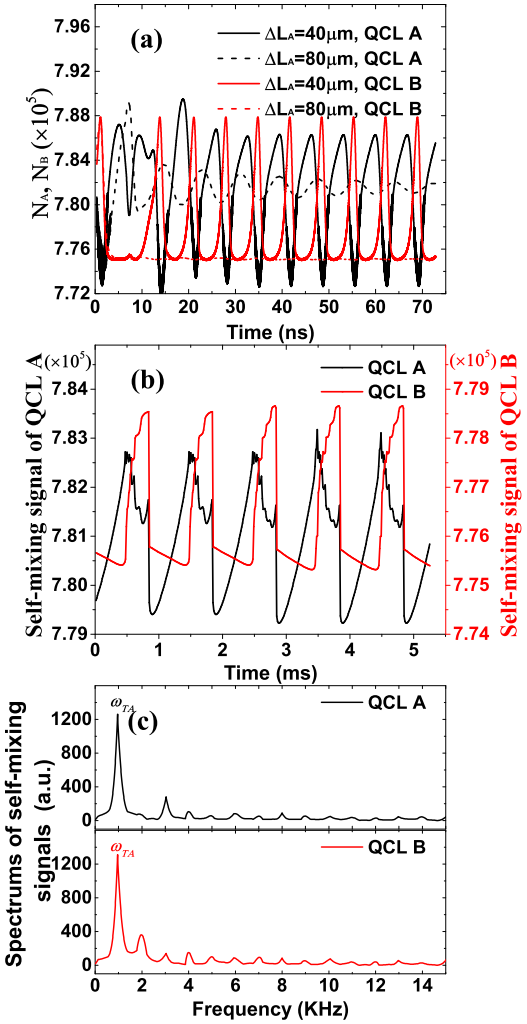

Fig. 4. For the case of strong feedback strength, the simulation with $\kappa_{OL} = 0.4\kappa_c$, $\Delta\Omega/2\pi = 0.16$ GHz. (a) Time evolution of $N_{A/B}$ with $\Delta L_A = 40\mu m$ and $\Delta L_A = 80\mu m$, (b) the self-mixing signals with the moving target $v_{TA} = 60$ mm/s, (c) spectrums of self-mixing signals.

as follows

$$\frac{d\varepsilon_B(t)}{dt} = i\Omega_{B0}\varepsilon_B(t) + \frac{1}{2}(1+i\alpha)\{Zg[N_{B,3}(t) - N_{B,2}(t)] - \frac{1}{\tau_p}\}\varepsilon_B(t) + \frac{\kappa_c}{\tau_l}\varepsilon_A(t-\tau_{ext}) + \frac{\kappa_{OR}}{\tau_l}\varepsilon_B(t-\tau_{OR}). \tag{17}$$

Then the phase-locked range is modified to $|\Delta\Omega|_{max} = (2\kappa_c + \kappa_{OL} + \kappa_{OR})\sqrt{1+\alpha^2}/\tau_l$, and the main peak frequency corresponding to target B in the self-mixing signal spectrums should be $\omega_{TB} = 2\Omega_L v_{TB}/c$. Figures 5(a) and 5(b) show the self-mixing signals and their spectrums in the phase-locked range with the frequency detuning $\Delta\Omega/2\pi = 0.1$GHz and κ_{OL}=$\kappa_{OR} = 0.1\kappa_c$. It is found that both spectrums of QCL A and QCL B include the main peaks corresponding to ω_{TA}, ω_{TB}, the difference frequency $\omega_{TB} - \omega_{TA}$, and the sum frequency $\omega_{TB} + \omega_{TA}$. The intensities

Optics EXPRESS

of the difference and sum frequency vary with the parameters of the lasers and the motion direction of the targets. Besides, we also simulate the situation that the array operates far from the phase-locked range with two moving targets, and the results are shown in Figs. 5(c) and 5(d) with $\Delta\Omega/2\pi = 10$GHz. It is found that the self-mixing signal of each laser only contains the velocity information of its corresponding target.

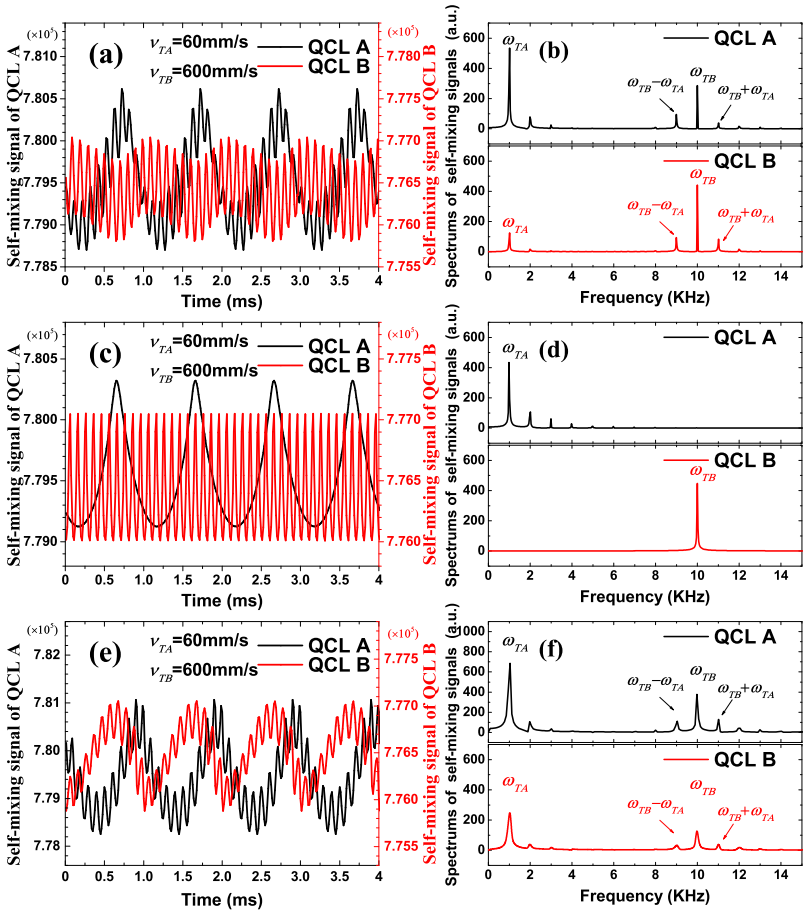

Fig. 5. Self-mixing signals and corresponding spectrums of QCLs A and B with two independent targets. (a)–(d) Simulations for the case in Fig. 1(b). (a) and (b) $\Delta\Omega/2\pi = 0.1$GHz, κ_{OL}=$\kappa_{OR} = 0.1\kappa_c$, (c) and (d) $\Delta\Omega/2\pi = 10$GHz, κ_{OL}=$\kappa_{OR} = 0.1\kappa_c$. (e)–(f) Simulations for the case in Fig. 1(c) with $\Delta\Omega/2\pi = 0.1$GHz, $\kappa_A = 0.1\kappa_c$, and $\kappa_B = 0.05\kappa_c$.

For the case of Fig. 1(c), the time evolution equations of the electric fields of the two lasers can be written as:

$$\frac{d\varepsilon_A(t)}{dt} = i\Omega_{A0}\varepsilon_A(t) + \frac{1}{2}(1+i\alpha)\{Zg[N_{A,3}(t) - N_{A,2}(t)] - \frac{1}{\tau_p}\}\varepsilon_A(t) + \frac{\kappa_c}{\tau_l}\varepsilon_B(t-\tau_{ext}) + \frac{\kappa_A}{\tau_l}\varepsilon_A(t-\tau_A) + \frac{\kappa_B}{\tau_l}\varepsilon_A(t-\tau_B), \tag{18}$$

$$\frac{d\varepsilon_B(t)}{dt} = i\Omega_{B0}\varepsilon_B(t) + \frac{1}{2}(1+i\alpha)\{Zg[N_{B,3}(t) - N_{B,2}(t)] - \frac{1}{\tau_p}\}\varepsilon_B(t) + \frac{\kappa_c}{\tau_l}\varepsilon_A(t-\tau_{ext}) + \frac{\kappa_B}{\tau_l}\varepsilon_B(t-\tau_B) + \frac{\kappa_A}{\tau_l}\varepsilon_B(t-\tau_A). \tag{19}$$

Optics EXPRESS

Fig. 5(e) shows the self-mixing signals of the THz QCLs array with $\Delta\Omega/2\pi = 0.1$GHz, $\kappa_A = 0.1\kappa_c$, and $\kappa_B = 0.05\kappa_c$. With such parameters, the array is phase-locked. The self-mixing signal spectrums are shown in Fig. 5(f). The main peaks corresponding to ω_{TA}, ω_{TB}, $\omega_{TB} - \omega_{TA}$, and $\omega_{TB} + \omega_{TA}$ can still be observed. The intensities of the peaks depend on the strengths of the mutual injection and the targets' feedbacks as well as the velocities of the targets, which is similar to the result of a solitary laser subjected to multi-targets' feedbacks [11].

These results indicate that self-mixing velocity sensor based on a mutual-injected THz QCL array can measure two independent targets simultaneously. Especially, for the phase-locked array, the motion information of all targets can be obtained by measuring the self-mixing signal of anyone of lasers in the array instead of analyzing all lasers.

4. Conclusion

In conclusion, the basic properties of mutual-injected THz QCL array with self-mixing feedback from an external moving target are studied theoretically. With weak feedback and small frequency detuning, the QCLs are phase-locked and each laser in the array can detect the velocity of the target. When the frequency detuning of the two lasers is too large, the array cannot be phase-locked and only the laser injected by the reflected light of the target can detect the target's velocity. Even for the case of strong feedback strength, the THz QCL array will not become extremely unstable and can still be used for the velocity measurements. The simultaneous measurement of two moving targets by the THz QCL array is also demonstrated. These results may be useful to the development of self-mixing interferometer with THz QCL arrays.

Funding

NSAF Joint Fund (U1730246); International Cooperation and Exchange Programme (F040302).

References

1. J. F. Federici, B. Schulkin, F. Huang, D. Gary, R. Barat, F. Oliveira, and D. Zimdars, "THz imaging and sensing for security applications—explosives, weapons, and drugs," Semicond. Sci. Technol. **20**(7), S266–S280 (2005).
2. P. H. Siegel, "Terahertz technology in biology and medicine," IEEE Trans. Microwave Theory Tech. **52**(10), 2438–2447 (2004).
3. W. L. Chan, J. Deibel, and D. M. Mittleman, "Imaging with terahertz radiation," Rep. Prog. Phys. **70**(8), 1325–1379 (2007).
4. B. S. Williams, "Terahertz quantum-cascade lasers," Nat. Photonics **1**(9), 517–525 (2007).
5. P. Dean, A. Valavanis, J. Keeley, K. Bertling, Y. L. Lim, R. Alhathlool, A. D. Burnett, L. H. Li, S. P. Khanna, D. Indjin, T. Taimre, A. D. Rakić, E. H. Linfield, and A. G. Davies, "Terahertz imaging using quantum cascade lasers—a review of systems and applications," J. Phys. D: Appl. Phys. **47**(37), 374008 (2014).
6. G. Giuliani, M. Norgia, S. Donati, and T. Bosch, "Laser diode self-mixing technique for sensing applications," J. Opt. A: Pure Appl. Opt. **4**(6), S283–S294 (2002).
7. F. P. Mezzapesa, L. L. Columbo, M. Brambilla, M. Dabbicco, S. Borri, M. S. Vitiello, H. E. Beere, D. A. Ritchie, and G. Scamarcio, "Intrinsic stability of quantum cascade lasers against optical feedback," Opt. Express **21**(11), 13748–13757 (2013).
8. B. Meng and Q. J. Wang, "Theoretical investigation of injection-locked high modulation bandwidth quantum cascade lasers," Opt. Express **20**(2), 1450–1464 (2012).
9. A. Valavanis, P. Dean, Y. L. Lim, R. Alhathlool, M. Nikolić, R. Kliese, S. P. Khanna, D. Indjin, S. J. Wilson, A. D. Rakić, E. H. Linfield, and A. G. Davies, "Self-mixing interferometry with terahertz quantum cascade lasers," IEEE Sens. J. **13**(1), 37–43 (2013).
10. R. Degl'Innocenti, R. Wallis, B. Wei, L. Xiao, S. J. Kindness, O. Mitrofanov, P. B. Weimer, S. Hofmann, H. E. Beere, and D. A. Ritchie, "Terahertz nanoscopy of plasmonic resonances with a quantum cascade laser," ACS Photonics **4**(9), 2150–2157 (2017).
11. F. P. Mezzapesa, L. L. Columbo, M. Dabbicco, M. Brambilla, and G. Scamarcio, "QCL-based nonlinear sensing of independent targets dynamics," Opt. Express **22**(5), 5867–5874 (2014).
12. L. K. Hoffmann, M. Klinkmüller, E. Mujagić, M. P. Semtsiv, W. Schrenk, W. T. Masselink, and G. Strasser, "Tree array quantum cascade laser," Opt. Express **17**(2), 649–657 (2009).
13. Y. Bai, S. Tsao, N. Bandyopadhyay, S. Slivken, Q. Y. Lu, D. Caffey, M. Pushkarsky, T. Day, and M. Razeghi, "High power, continuous wave, quantum cascade ring laser," Appl. Phys. Lett. **99**(26), 261104 (2011).

Optics EXPRESS

14. T.-Y. Kao, J. L. Reno, and Q. Hu, "Phase-locked laser arrays through global antenna mutual coupling," Nat. Photonics **10**(8), 541–546 (2016).
15. Y. Halioua, G. Xu, S. Moumdji, L. Li, J. Zhu, E. H. Linfield, A. G. Davies, H. E. Beere, D. A. Ritchie, and R. Colombelli, "Phase-locked arrays of surface-emitting graded-photonic-heterostructure terahertz semiconductor lasers," Opt. Express **23**(5), 6915–6923 (2015).
16. A. Khalatpour, J. L. Reno, and Q. Hu, "Phase-locked photonic wire lasers by π coupling," Nat. Photonics **13**(1), 47–53 (2019).
17. N. Rothbart, H. Richter, M. Wienold, L. Schrottke, H. T. Grahn, and H.-W. Hübers, "Fast 2-D and 3-D terahertz imaging with a quantum-cascade laser and a scanning mirror," IEEE Trans. Terahertz Sci. Technol. **3**(5), 617–624 (2013).
18. Y. Li, N. Yang, Y. Xie, W. Chu, W. Zhang, S. Duan, and J. Wang, "Basic phase-locking, noise, and modulation properties of optically mutual-injected terahertz quantum cascade lasers," Opt. Express **27**(3), 3146–3160 (2019).
19. E. A. Viktorov, A. M. Yacomotti, and P. Mandel, "Semiconductor lasers coupled face-to-face," J. Opt. B: Quantum Semiclassical Opt. **6**(2), L9–L12 (2004).
20. F. Rogister and J. García-Ojalvo, "Symmetry breaking and high-frequency periodic oscillations in mutually coupled laser diodes," Opt. Lett. **28**(14), 1176–1178 (2003).
21. L. Junges, A. Gavrielides, and J. A. C. Gallas, "Synchronization properties of two mutually delay-coupled semiconductor lasers," J. Opt. Soc. Am. B **33**(7), C65–C71 (2016).
22. N. Jiang, W. Pan, L. Yan, B. Luo, W. Zhang, S. Xiang, L. Yang, and D. Zheng, "Chaos synchronization and communication in mutually coupled semiconductor lasers driven by a third laser," J. Lightwave Technol. **28**(13), 1978–1986 (2010).
23. R. Lang and K. Kobayashi, "External optical feedback effects on semiconductor injection laser properties," IEEE J. Quantum Electron. **16**(3), 347–355 (1980).
24. T. Gensty and W. Elsäßer, "Semiclassical model for the relative intensity noise of intersubband quantum cascade lasers," Opt. Commun. **256**(1-3), 171–183 (2005).
25. Y. Petitjean, F. Destic, J. C. Mollier, and C. Sirtori, "Dynamic modeling of terahertz quantum cascade lasers," IEEE J. Sel. Top. Quantum Electron. **17**(1), 22–29 (2011).
26. X. Qi, G. Agnew, I. Kundu, T. Taimre, Y. L. Lim, K. Bertling, P. Dean, A. Grier, A. Valavanis, E. H. Linfield, A. G. Davies, D. Indjin, and A. D. Rakić, "Multi-spectral terahertz sensing: proposal for a coupled-cavity quantum cascade laser based optical feedback interferometer," Opt. Express **25**(9), 10153–10165 (2017).
27. R. P. Green, J. H. Xu, L. Mahler, A. Tredicucci, F. Beltram, G. Giuliani, H. E. Beere, and D. A. Ritchie, "Linewidth enhancement factor of terahertz quantum cascade lasers," Appl. Phys. Lett. **92**(7), 071106 (2008).
28. C. Wang, F. Grillot, V. Kovanis, and J. Even, "Rate equation analysis of injection-locked quantum cascade lasers," J. Appl. Phys. **113**(6), 063104 (2013).
29. S. Kumar, B. S. Williams, S. Kohen, Q. Hu, and J. L. Reno, "Continuous-wave operation of terahertz quantum cascade lasers above liquid-nitrogen temperature," Appl. Phys. Lett. **84**(14), 2494–2496 (2004).
30. B. S. Williams, S. Kumar, Q. Hu, and J. L. Reno, "Operation of terahertz quantum-cascade lasers at 164 K in pulsed mode and at 117 K in continuous-wave mode," Opt. Express **13**(9), 3331–3339 (2005).

158.0.232.51 on 2022-07-01 04:37:02